Advantages and Disadvantages of His-Tagged Beta-Galactosidase

Sandra S. Flores
Universidad Nacional de Cordoba Facultad de Ciencias Exactas Fisicas y Naturales. ICTA. Depto de Química. CONICET. Instituto de Investigaciones Biológias y Tecnologicas IIByT

Pedro D. Clop
Universidad Nacional de Cordoba Facultad de Ciencias Exactas Fisicas y Naturales. ICTA. Depto Química. CONICET. Instituto de Investigaciones Biológicas y Tecnológicas. IIByT

José L. Barra
Universidad Nacional de Córdoba. Facultad de Ciencias Químicas. Depto de Química Biológica Ranwell Caputto. Centro de Investigaciones en Quimica Biologica de Córdoba

Carlos Argaraña
Universidad Nacional de Cordoba Facultad de Ciencias Quimicas. Depto. de química Biológica Ranwell Caputto. CONICET. Centro de Investigaciones en Química Biológica. CIQUIBIC

María A. Perillo
Universidad Nacional de Córdoba. Facultad de Ciencias Exactas Físicas y Naturales. ICTA. Depto de Química. CONICET. Instituto de Investigaciones Biológicas y Tecnológicas. IIBYT

Verónica Nolan
Universidad Nacional de Córdoba. Facultad de Ciencias Exactas, Físicas y Naturales. ICTA. Depto de Química. CONICET. Instituto de Investigaciones Biológicas y Tecnológicas. IIByT

Julieta M. Sanchez (julieta.sanchez@unc.edu.ar)
Consejo Nacional de Investigaciones Cientificas y Tecnicas y Universidad Nacional de Córdoba
https://orcid.org/0000-0001-6676-5776

Research

Keywords: beta-galactosidase, His-tag, enzymatic activity, protein structure, thermal stability

Posted Date: August 17th, 2020

DOI: https://doi.org/10.21203/rs.3.rs-54150/v1

Advantages and disadvantages of His-tagged beta-galactosidase

Sandra S Flores[1,2], Pedro D. Clop[1,2], José L. Barra[3,4], Carlos E. Argaraña[3,4], María A. Perillo[1,2], Verónica Nolan[1,2]* and Julieta M. Sánchez[1,2]*

[1]*Universidad Nacional de Córdoba, Facultad de Ciencias Exactas, Físicas y Naturales. ICTA and Departamento de Química, Cátedra de Química Biológica. Av. Vélez Sarsfield 1611, 5016 Córdoba, Argentina.*

[2] *CONICET, Instituto de Investigaciones Biológicas y Tecnológicas (IIByT). Córdoba, Argentina.*

[3]*Universidad Nacional de Córdoba, Facultad de Ciencias Químicas, Departamento de Química Biológica "Ranwel Caputto". Av. Haya de la Torre s/N° Ciudad Universitaria CP. X5000HUA Córdoba, Argentina.*

[4]*CONICET, Centro de Investigaciones en Química Biológicas de Córdoba (CIQUIBIC), Córdoba, Argentina.*

*Corresponding authors

vnolan@unc.edu.ar

julieta.sanchez@unc.edu.ar

Abstract

β-Galactosidase is one of the most important biotechnological enzyme used in the dairy industry, pharmacology and in molecular biology. In our laboratory we have overexpressed a recombinant β-galactosidase in *Escherichia coli* (*E. coli*). This enzyme differs from its native version (β-Gal_{WT}) in that 6 histidine residues have been added to the carboxyl terminus in the primary sequence (β-Gal_{His}), which allows its purification by immobilized metal affinity chromatography (IMAC). In this work we compared the functionality and structure of both proteins and evaluated their catalytic behavior on the kinetics of lactose hydrolysis. We observed a significant reduction in the enzymatic activity of β-Gal_{His} with respect to β-Gal_{WT}. Although, both enzymes showed a similar catalytic profile as a function of temperature, β-Gal_{His} presented a higher resistance to the thermal inactivation and evidenced greater half-life time compared to β-Gal_{WT}. At room temperature, β-Gal_{His} showed a fluorescence spectrum compatible with a partially unstructured protein however, it exhibited a lower tendency to the thermal-induced unfolding with respect to β-Gal_{WT}. Analytical ultracentrifugation experiments demonstrated that the population of β-Gal_{His} molecules exhibited a higher proportion of monomers and a lower proportion of tetrameric species with respect to the His-tag free protein. The impairment of tetramerization may would explain the negative effect of the presence of His-tag on the enzymatic activity. In addition, the present results, analyzed in the context of the available literature, suggest that the effect of the His-tag is protein-specific.

Keywords

beta-galactosidase, His-tag, enzymatic activity, protein structure, thermal stability.

1.Introduction

β-D-galactosidase [EC 3.2.1.23] (β-Gal) is a glycoside hydrolase enzyme that catalyzes the hydrolysis of glycosidic bonds, producing monosaccharides from β-galactosides [1]. β-Gal has been extensively studied because of its nutritional, biotechnological and therapeutic impact [2,3]. In our laboratory, we are interested in describing how the recombinant production of proteins, particularly β-Gal, and the purification strategies could modulate their structure/function relationship.

Within the vast alternatives of biological systems for recombinant protein production, *E. coli* is the preferred microorganism for protein expression because of the easy handling and storage [4]. Besides, in the protein purification step, histidine tags (His-tag) have gained great popularity [5,6]. His-tags (typically containing six or more consecutive histidine residues) may be used for protein purification by immobilized metal affinity chromatography (IMAC), where divalent cations (usually Ni^{2+} or Co^{2+}) are adsorbed in an agarose matrix. The first report on using the nickel coupled to nitriloacetic acid agarose system (Ni^{2+}-NTA) for His-tag protein purification was dated on 1975 [7]. His-tag protein goes through the agarose column and attach to it. In principle, the basic nitrogen atom in the imidazole of histidine has an alone electron pair that coordinate with metallic cations (Ni^{2+}) [8]. Also, nonspecific interactions, e.g., electrostatic and hydrophobic forces contribute to protein-agarose binding. Then histidine or imidazole have been applied as elution agents for immobilized metal affinity displacement chromatography [9].

In some cases, the tags also help in protein expression, folding, and/or solubility [10,11]. For instance, *in vitro* designed oligomeric proteins have been engineered through the interaction of His-tag with divalent cations as protein biomaterial with novel therapeutic properties [12]. Moreover, a family of metal-NTA based fluorescence probes has been developed for the intracellular visualization of His-tag proteins [13]. Immobilized metal affinity (IMA) strategy was also used to study protein-membrane interaction. Raghunath et al. studied the kinetics of His-tag protein binding to nickel decorated liposomes. They found that protein-membrane association involves the binding and reorganization of protein conformation according to an increase in the membrane packing. This approach allows to describe the intermediates preceding membrane bending driven by protein crowding [14].

It is usually accepted that due to their small size, His-tags would not interfere with the function and structure of the majority of proteins [10,15]. However, there is an increase number of reports showing that this conception may be not always true [16–18]. Moreover, there are evidences that His-tags may affect the oligomeric states of proteins as well as their function [19–21]

In the present study we compared a β-Gal containing a hexahistidine peptide added in the C-terminal, β-Gal$_{His}$, with its wild type commercial counterpart, β-Gal$_{WT}$. Our results contributed to understand the unique effects of His-tag in proteins.

2. Materials and Methods

2.1. Materials.

Luria-Bertani medium (LB). Isopropyl-β-D-thiogalactopyranoside (IPTG), Kanamycin Sulfate (Sigma Aldrich); *Escherichia coli* K-12 W3110, *Escherichia coli* strain BL 21λCodon plus (Novagen)

Other reagents and solvents were of analytical grade.

2.2. Methods.

2.2.1. Cloning β-Gal gene.

The β-galactosidase gene was amplified from *E. coli* K-12 W3110 genomic DNA by PCR using primers Bgal S1N (5'-CATATGACCATGATTACGGATTCACTGGCCGTCGTTTTACAACGTCG-3') and BgalA1 (5'- GGCTCGAGTTTTTGACACCAGACCAACTGGTA-3') the PCR products were partially digested with NdeI and Xho I and inserted into pET26b (+) using the same restriction enzymes, yielding the plasmid pET 26+βgal which contains a C-terminal six histidine tag sequence[22].

2.2.2.β-Gal Expression and Purification.

Escherichia coli strain BL21λCodon plus (Novagen) transformed with Plasmid pET 26+βgal was grown at 37°C in Luria-Bertani medium (LB) supplemented with kanamycin 50 µg/ml[22]. β-Gal expression was induced adding isopropyl-β-D-thiogalactopyranoside (IPTG) to a final concentration of 0.4 mM at OD_{600} of approximately 0.6 and further incubation at 20°C for 20 h. The grown cells were harvested by centrifugation at 5,000 g for 20 min at 4ºC, resuspended in 20 mL of NaCl 500 mM in phosphate buffer 0.05 M, pH 6.8. Then the cells were incubated with lysozyme (0.3 mg/mL) for 30 min. at 20°C. After that, bacteria were disrupted by three cycles of sonication of 30 seconds each, frozen with liquid nitrogen

and thawed in a water bath at 35ºC. Then, the lysed cells were centrifuged at 10000 rpm for 30 min. at 4°C and the supernatant was then incubated with 1 mL Ni-NTA beads (ProBond™ resin Invitrogen) for 3h at 4ºC by tumbling. Then the beads were poured in cartridges and washed with imidazole solution of 0, 60, 100, 200 and 400 mM. Each elution sample was dialyzed against 0.05 M phosphate buffer (pH 6.8) at 4ºC for 20 h with 3-4 changes of buffer.

The sample eluted with the 200 mM imidazole contained a considerable amount of highly pure β-Gal tested by SDS-PAGE and finally the pure enzyme was stored at 4ºC in dialysis buffer (at 3 mg/mL).

β-Gal SDS-PAGE

The β-Gal purity was evaluated by sodium dodecyl sulfate polyacrylamide gel electrophoresis (SDS-PAGE) (10%). Samples were heated at 100 °C during 5 min. in loading buffer[23]. The ammount of protein submitted to SDS-PAGE was around 90 µg. After running, the proteins in the gel were stained with coomassie blue.

2.2.4. Protein quantitation.

Protein concentration was measured by the Lowry's method [24].

2.2.3.β-Gal activity assay.

2.2.3.1. Determination of kinetic parameters.

The reaction was carried out in phosphate buffer 0.05 M, pH 6.8 using monohydrated Lactose (Anedra) as substrate. It was initiated by the addition of 0.01 mL of the enzyme preparation containing (0.001 mg to 0.01 mg of β-Gal) and incubated for 20 min at 37°C. Then, the reaction was quenched by boiling 5 min. β-Gal activity was measured by quantitative analysis of the glucose released, determined by the glucose oxidase method [25]. One unit of enzyme activity was defined as the amount of enzyme required to produce 1 µmol of glucose/min in the described conditions.

The values of K_M and V_{max} were determined by fitting the Michaelis–Menten equation to the *V*o versus substrate concentration data plot by a computer aided nonlinear regression analysis.

2.2.3.2. Temperature-dependent β-Gals activity profile.

The thermal activity profiles of β-Gal_{WT} and β-Gal_{His} were evaluated from 25°C to 65°C at pH 6.8. The other reaction conditions were described above.

2.2.3.3. Thermal stability of β-Gals.

The thermal stability of β-Gal_{WT} and β-Gal_{His} was studied by measuring the residual catalytic activity determined as described above after a pre-incubation period of 20 min. at different temperatures (20 - 60ºC).

2.2.3.4. Half-life time.

Residual activity was measured as described above, a closed cap tube containing 3 µl of β-Gal (0.01 g/L), preincubated at 50ºC during a time ranging from 2 to 20 min. After this time, 300 µl of lactose (200 mM) was added and the specific enzyme activity was measured as described above at 37º. The profile of residual activity was plotted vs time.

A single exponential decay mathematical approach was applied to fit the curve of specific activity (SA) vs time, in order to determine the half-life time ($\tau_{1/2}$).

$$SA_{0.5} = SA_{initial} \times e^{-k} \quad (1)$$

$$\frac{SA_{0.5}}{SA_{initial}} = e^{-k\tau} \quad (2)$$

$$ln\ 0.5 = -k\tau_{1/2} \quad (3)$$

$$\tau_{1/2} = \frac{0.69}{k} \quad (4)$$

where $SA_{initial}$ is the specific activity measured at zero time, $SA_{0.5}$ is the half value of $SA_{initial}$, k is the constant of exponential decay, and $\tau_{1/2}$ is the half-life time.

157

158 *2.2.5. Structural properties of β-Gals.*

159 *2.2.5.1. Fluorescence spectroscopy.*

160 Fluorescence spectra were recorded in a Fluoromax Spex-3 JovinYvon (Horiba, New Jersey, USA)
161 spectrofluorimeter. A quartz cell with 10 mm path length and a thermostated holder was used. The slits
162 and λ_{ex} were set at 2 nm and 290 nm, respectively. Emission spectra were acquired within the 300-400
163 nm range. Protein concentration used was 0.2 mg/ml. Raman scattering contribution from water was
164 subtracted in all spectra. To facilitate comparisons, λ_{max} was determined but also the center of spectral
165 mass (CSM) was calculated for each fluorescence emission spectra [26] according to equation (5), where
166 I_i is the absorbance or the fluorescence intensity measure at the wavelength λ_i.

167

168 $$\lambda = \frac{\sum \lambda_i . I_i}{\sum I_i} \qquad (5)$$

169

170 We also analyzed the λ_{max} from each protein vs temperatures within 20 to 60 ºC range. At rate heating
171 of 1ºC/min.

172

173 *2.2.5.2. Analytical ultracentrifugation (AUC).*

174 β-Gals (0.5 mg/mL) solutions prepared in 0.05 M phosphate buffer, pH 6.8 were submitted to
175 Sedimentation Velocity (SV) analysis as described previously [27]. Briefly, it was carried out with an
176 Optima XL-A analytical ultracentrifuge (Beckman Coulter Inc., Fullerton, CA, USA) equipped with a
177 spectrometric UV-visible system. All SV experiments were conducted at 40,000 rpm at 20°C; 50 scans
178 were recorded along 2 h, at 280 nm. The reference cell contained buffer solution. To obtain the
179 sedimentation coefficient (S) of each species, data were analyzed with SEDFIT software, using the
180 continuous sedimentation coefficient distributions c(s) model [28].The experimental s-value were
181 transformated into a value under standard conditions (water 20ºC). The viscosity and density values
182 (required for S calculations) in the case of β-Gal solutions were determined using SEDNTERP software
183 [29]. *S* has the dimensions of time units expressed in Sverdberg ($1S=10^{-13}$s) and can be calculated by
184 equations (6) and (7)

$$v_t = \frac{M.r.\omega^2}{6.\pi..r_0} \quad (6)$$

$$S = \frac{v_t}{r.\omega^2} = \frac{M}{6.\pi..r_0} v_t = \frac{m.r.\omega^2}{6.\pi..r_0} v_t = \frac{m.r.\omega^2}{6.\pi..r_0} \quad (7)$$

where v_t is the sedimentation rate, r is the distance of the particle from the axis of rotation, M the molar mass of the particle and ω is the angular velocity of the rotor equation (6). S serves to normalize the v_t of a particle by the acceleration applied to it ($r.\ \omega^2$). The resulting value is independent on the acceleration but depends on the properties of the particle (the mass m and the hydrodynamic radius r_0) and the viscosity of the medium (η) where it is suspended as shown by equation (7). Experimentally, the absorbance profile obtained by analytical ultracentrifugation is described by the Lamm equation equation (8) and S can be calculated:

$$\frac{d[\beta Gal]}{dt} = \frac{1}{r}\frac{d}{dr}\left[rD(M)\frac{d[\beta Gal]}{dr} - S(M)\omega^2 r^2[\beta Gal]\right] \quad (8)$$

where *D(M)* is de diffusion coefficient which, as well as *S(M)*is dependent on the molar mass (M) of the particle (in this case the β-Gal molecule).

2.6 Statistical calculations.

The least squares method was applied to fit functions through nonlinear regression analysis. Pairwise comparisons were made with the Student`s t-test using Sigma Plot version 12.5.

3. Results and Discussion.

3.1. β-Gals functionality.

In most cases, the incorporation of His-tag has resulted in great increases in the efficiency of the protein purification process however, sometimes, it hampers the protein functionality. Then, several experiments were conducted to remove the additional histidine residues but drawbacks remain if non-wild type amino acids remain in the protein [18]. In our experiments we evaluate the enzymatic activity of the wild type β-Gal$_{WT}$, the commercial enzyme from Sigma, and a recombinant β-Gal$_{His}$ that we

produced and purified by IMAC chromatography. Both enzymes show a michaelian behavior. However, β-Gal_{His} exhibits lower specific activity with respect to β-Gal_{WT} (Fig.1, Table 1); a V_{max} decrease of around 60 % is observed for β-Gal_{His} with respect to β-Gal_{WT}. On the other hand, the presence of histidine residues also seems to moderately favor the affinity of the active sites for lactose (β-$Gal_{His}K_M$ < *β*-$Gal_{WT}K_M$), although, the difference observed in the later parameter was not statistically significant. We ruled out the possibility that the difference in the kinetic parameters were due to impurities in the protein sample. SDS-PAGE (Fig 1.b) showed that both samples only present the β-gal monomer (116 kD) band.

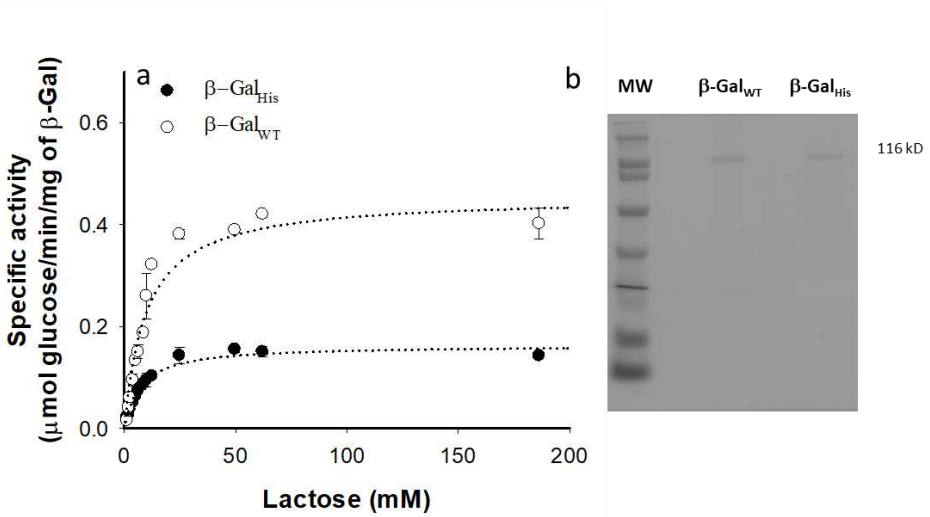

Fig. 1 Functional β-Gal properties. a) Specific activity as a function of lactose concentration (β-Gal_{WT} white symbols, β-Gal_{His}, black symbols). Samples were incubated for 20 min, at 37°C and pH 6.8 and all measurements were carried out in conditions of initial velocity, according to Michaelis-Menten (MM) model. Hyperbolic curves could be adjusted to the experimental points, according to the MM equation. The resulting kinetic parameters are shown in Table 1.b) β-Gals SDS-PAGE.

Table 1. Kinetic and structural parameters for β-Gal_{His} and β-Gal_{WT}

		β-Gal_{His}	β-**Gal_{WT}**
Kinetic parameters	**Vmax** (µmol/min/mg)	0.163 ± 0.005*	**0.46** ± 0.02*
	K_M (mM)	7.27 ± 0.73	9.9 ± 1.5
Structural parameters	**$\tau_{1/2}$**(min)	8.1 ± 1.2#	5.6 ± 0.9#
	λ_{max}(nm)	347	345

	CSM (nm)	360	356

Vmax, K_M and $\tau_{1/2}$ values are the mean ± sem. *statistically significant difference (P = <0.001).#statistically significant difference (P = 0.045).

Firstly, we decided to add the His-tag at the carboxyl terminus of β-Gal because the amino terminus of the protein takes part of the active site [30], in spite of the fact that Brome and her colleagues expressed an active β-Gal with the His-tag in the amino terminal of the primary sequence [31]. Besides, Ullman [32] found β-Gal activity in hybrid proteins where tags appeared localized in both extremes of the sequence. In those cases, any structure-function analysis nor any comparison to the wild type protein was developed to describe the tags effects on the protein.

For other proteins, there are differences on the molecular performance according to the location of the His-tag within the protein sequence [33,34]. For instance, the rat corticotropin-releasing factor receptor type 2a adopts two different disulfide bond patterns at the N-terminus when the His-tag is at either the N- or C-terminal [35].

Otherwise, the effect of His-tag on protein function is varied according with the protein. In GNAT superfamily, the His-tag binds at the substrate site and acts as a weak competitive inhibitor for the substrate [17]. On the other hand, the lower catalytic efficiency of the His-tagged with respect to the wild type chondroitinase ABC-I was related with the difficult to completely degrade the chondroitin sulfate to low molecular weight products [36] .

Beyond the diminution we observed in the enzymatic activity, we investigated if the His-tag affected the thermal properties of β-Gal. For that, different approaches were used: a) the temperature effect on enzyme activity, b) the resistance to thermal inactivation and c) the half-life time for the enzyme denaturation. Results are shown in Fig. 2 and Table 1. Both enzymes exhibit the same catalytic profile vs reaction temperature with an optimal activity at around 45°C (Fig. 2a). Moreover, the negative effect of high temperature was much more important for the wild type than for the His-tagged enzyme: when the enzymatic activity is measured at 50°C, β-Gal_{His} maintains approximately 50% while β-Gal_{WT} only exhibits around 20 % of the optimal activity. In terms of thermal stability, β-Gal_{His} presents a higher

resistance to temperature inactivation compared to β-Gal_{WT} as shown in Fig. 2b. In order to evaluate this difference, the half-life time of each enzyme (Fig. 2c) was studied. The preincubation of the enzymes at 50ºC β-Gal_{His} reflects this tendency and β-Gal_{His} seems to be more stable with respect to β-Gal_{WT} (Table 1). The effect of His-tag on proteins thermal stability is different depending on the protein but in general, a negative effect is observed. Chen and his collaborators [36] found that the presence of a His-tag produced a particular result in the choindroitinase ABC1 (ChSase ABC I) thermal response. Their results demonstrated that His-tag could improve the thermostability of ChSase ABC I when it was incubated at relative low temperatures (30°C-35°C), but the opposite effect occurs at high temperatures (40°C-45°C). On the other hand, Booth and coworkers [18] using differential scanning fluorimetry studied the thermostability for a set of ten different N-Terminal His-tagged proteins and found that in almost all cases, the His-tagged version was less stable than the wild type protein.

This scenario encourages us to explore the structural features underlying the differential behavior of β-Gal_{WT} and β-Gal_{His}.

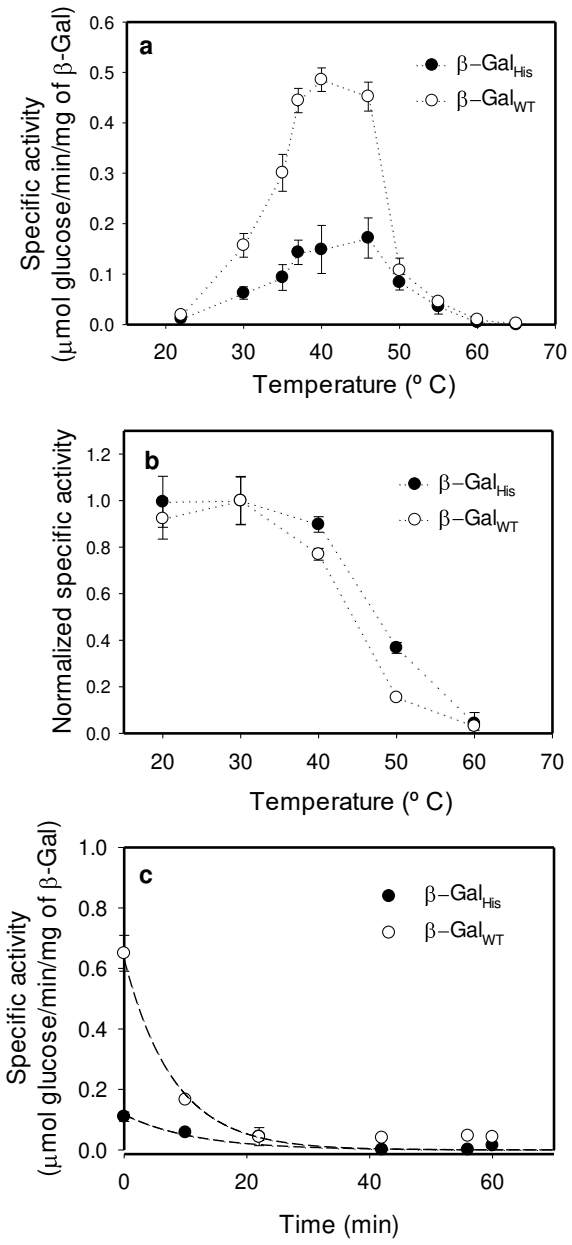

Fig. 2. Thermal and temporal inactivation profiles of β-Gals.a) Specific activity measured at the indicated temperature within the range 22ºC - 65ºC. b) β-Gal specific activity measured at 37ºC after preincubation for 20 min. at different temperatures (20-60ºC). In each data set normalization was done with respect to the corresponding specific activity preincubated at 30ºC, which was taken as the unity. c) Catalytic activity was evaluated at 37ºC, pH 6.8 and lactose 200 mM after preheating the proteins (0.01 g/L) at 50ºC during a fix time period (20-60 min). Exponential decay curves (dashed lines) are the fitness to the experimental points (black and white circles) and allowed estimating the half-life times (shown in Table 1).

276

277 3.2. Structural properties of β-Gals.

278 3.2.1. Fluorescence Spectroscopy.

279 The fluorescence emission of Trp is sensitive to the polarity of the environment and can be used to detect
280 conformational changes in proteins [26]. β-Gal is a tetrameric protein with 39 Trps residues per protomer
281 [30]. β-Gal_{WT} fluorescence spectrum shows a λ_{max} at 345 nm and CSM=356 nm (Fig.3a, Table 2) which is
282 compatible with Trp residues localized in highly polar environment if compared with the spectrum of
283 Trp localized in a buried or non-polar medium (λ_{max}~325 nm). It is noteworthy that we tested the Mg^{2+}
284 free protein. This condition could contribute to the higher value of λ_{max} in β-Gal_{WT} spectrum compared
285 to those previously reported for the same protein[37]. For β-Gal_{His}, the spectrum shows an important
286 bathocromic shift, with a λ_{max} at 347 nm and CSM=360 nm (Fig. 3a, Table1). These results indicate that
287 Trp residues became, on average, more accessible to the solvent and that the His-tag could induce at
288 least a partial unfolding of β-Gal or, on average, a highly hydrated structure.

289 However, when λ_{max} was evaluated along heating (Fig. 3b) we observe that the His-tagged protein shows
290 a greater thermal stability with respect to the wild type protein (compare the magnitude of the thermal
291 λ_{max} increase up to 50ºC in both samples). In our laboratory we have also described an increase in the
292 thermal stability of β-Gal_{WT} when interacting with model membranes or in molecular crowded
293 conditions [37,38]. The present results indicate that the covalent modification on β-Gal_{WT} leading to β-
294 Gal_{His} also accounts for the increase resistance to inactivation that displays the latter compared with the
295 former (Fig. 2b). Moreover, at 50ºC and above we observe the major differences in the λ_{max} value
296 between both proteins. It is noteworthy that at 50ºC β-Gal_{His} shows lower values of λ_{max} with respect to
297 β-$Gal_{WT.}$ and as consequence, an opposite structural behavior respect to what was observed at 25ºC.

298

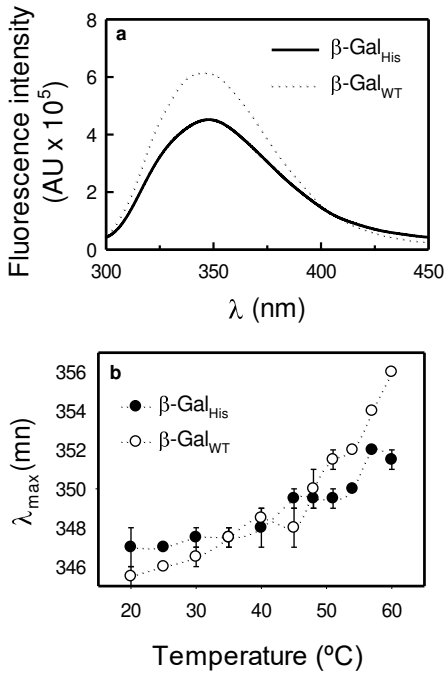

299

300 **Fig. 3. Structural analysis of β-Gals** a) Intrinsic fluorescence spectra of of β-Gal$_{His}$ (dotted line) and
301 β-Gal$_{WT}$ (full line) proteins at 0.2 g/L at 25°C. b) Effect of temperature on the λ_{max} of β-Gal$_{His}$ (●) and
302 β-Gal$_{WT}$ (○).

303

304 The most active form of β-Gal$_{WT}$ have been described when the protein oligomerized as a tetramer [39]. It
305 is well documented that the decrease of the tetramer in favor of minor oligomeric states could lead to a
306 negative effect in β-Gal functionality [40,41]. However, a superactive molecule could be observed when
307 higher oligomeric and/or particulated forms of the enzyme are present in the sample [22,42]. On the other
308 hand, Wu and Filutowics [43] proposed that His tagged proteins may differ from their wild type
309 counterparts in dimerization/oligomerization and afterwards, many researchers lead to similar
310 conclusion. Also, His-tag promoted the dimerization of HSC70 $_{C30\Delta L}$-His but had no effect on the elution
311 profile of HSC70 C30$_{WT}$-His(+), compared to their respective untagged forms [44]. Moreover, Kenig and
312 her colleagues [45] demonstrated that the His-tagged proteins were located intracellularly as soluble
313 proteins and also in an aggregated form as inclusion bodies. In contrast, the non-tagged proteins were
314 found only in the soluble form and this fraction was used for further purification studies. With those
315 concepts in mind we decided to evaluate the oligomeric state of our β-Gals.

316

317 3.2.2. Analytical ultracentrifugation (AUC)

318 In order to evaluate the effect of His-tag on the supramolecular organization of the enzyme we developed
319 AUC. Both enzymes presented a heterogeneous profile, but the presence of histidine seems to increase
320 the population of monomers (Table 2, Fig.4). Besides, it was remarkable the lower proportion of the
321 tetramers' population found in Gal_{His} if compared with β-Gal_{WT}. These phenomena contribute to explain
322 the negative effect of the presence of a His-tag on the enzyme activity.

323

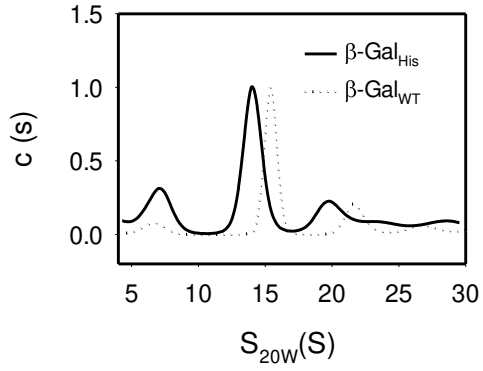

324

325 **Fig. 4. Analytic ultracentrifugation** of β-Gal_{His} (full line) and β-Gal_{WT} (dotted line)

326

327

328 **Table 2. Data from AUC hprofile from each β-Gal**

	β-Gal_{His}		β-Gal_{WT}	
Supramolecular organization	**%**	**Size (kD)**	**%**	**Size (kD)**
monomer	**15.1**	115.7	7.2	106.6
tetramer	39.2	333.4	**49.3**	387.8
Oligomer 1	**20.7**	626.7	16.7	656.9
Oligomer 2	8.6	998.9	8.5	904.3
*Oligomer 3**	16.1	1300-3001	18.2	1141-1740

329 *Correspond to the sum of all the oligomers bigger than 1141 kD that appear in the AUC data

Another important finding was the lower size (or hydrodynamic radius) of the β-Gal_{His} tetramer if compared with that of β-Gal_{WT} which may also be associated with an inactive conformational structure of the protein. All these results could explain the decreased in His-tagged protein functionality. This statement is supported by the fact that the active site is made up of elements from two subunits of the tetramer, and disassociation of the tetramer into dimers removes critical elements of the active site[30].

4. Conclusions

In the present work, through kinetic, fluorometric and ultracentrifugation analysis, we demonstrated that the addition of a His-tag to *E. coli* β-Gal reduces the catalytic activity possibly through an impairment of the proper acquisition of the typically active quaternary structure (tetramers). However, the tendency to form higher oligomeric structures may explain the improvement in the thermal structural and functional stability. It is important to consider that, in view of the present study and the available literature, the effect of His-tag seems to be protein-specific.

Declarations

Ethics approval and consent to participate

Not applicable

Consent for publication

Not applicable

Availability of data and materials

The datasets during and/or analysed during the current study available from the corresponding author on reasonable request.

Competing interests

The authors declare that they have no competing interests

Funding

This work was partially financed by SeCyT-Universidad Nacional de Córdoba and CONICET from Argentina.

Authors' contributions

Autor contributions statements

Flores, Sandra S. Investigation, writing, editing methodology and formal analysis

Clop, Pedro D. Investigation, writing, editing and formal analysis

Barra, José Investigation, writing, editing and formal analysis

Argaraña, Carlos Investigation, writing and editing

Perillo, Maria A. Investigation, writing and editing

Nolan, María V. Conceptualization, writing and editing

Sanchez, Julieta M. Conceptualization, writing and editing and supervision

Acknowledgements

All authors are members of the later institution and professors at the Universidad Nacional de Córdoba except SF who holds a fellowship from CONICET. Sedimentation velocity analysis were performed in the *Analytical Ultracentrifugation Laboratory* from IIBYT(CONICET-UNC).

REFERENCES:

1. Kayukawa CTM, Oliveira MAS, Kaspchak E, Sanchuki HBS, Igarashi-Mafra L, Mafra MR. Quillaja bark saponin effects on Kluyveromyces lactis beta-galactosidase activity and structure. *Food Chem*. 2020;303:125388. doi:https://doi.org/10.1016/j.foodchem.2019.125388
2. Husain Q. Beta-Galactosidases and their potential applications: A review. *Crit Rev Biotechnol*. 2010;30:41-62. doi:10.3109/07388550903330497

3. Cai Y, Zhou H, Zhu Y, et al. Elimination of senescent cells by beta-galactosidase-targeted prodrug attenuates inflammation and restores physical function in aged mice. *Cell Res*. Published online 2020. doi:10.1038/s41422-020-0314-9
4. Rosano GL, Ceccarelli EA. Recombinant protein expression in Escherichia coli: advances and challenges. *Front Microbiol*. 2014;5:172. doi:10.3389/fmicb.2014.00172
5. Kimple ME, Brill AL, Pasker RL. Overview of Affinity Tags for Protein Purification. *Curr Protoc Protein Sci*. 2013;73(1):9.9.1-9.9.23. doi:10.1002/0471140864.ps0909s73
6. Zeng K, Sun E-J, Liu Z-W, et al. Synthesis of magnetic nanoparticles with an IDA or TED modified surface for purification and immobilization of poly-histidine tagged proteins. *RSC Adv*. 2020;10:11524-11534. doi:10.1039/c9ra10473a
7. Porath J, Carlsson JAN, Olsson I, Belfrage G. Metal chelate affinity chromatography, a new approach to protein fractionation. *Nature*. 1975;258(5536):598-599. doi:10.1038/258598a0
8. Liao S-M, Du Q-S, Meng J-Z, Pang Z-W, Huang R-B. The multiple roles of histidine in protein interactions. *Chem Cent J*. 2013;7(1):44. doi:10.1186/1752-153x-7-44
9. Chen W-Y, Wu C-F, Liu C-C. Interactions of Imidazole and Proteins with Immobilized Cu(II) Ions: Effects of Structure, Salt Concentration, and pH in Affinity and Binding Capacity. *J Colloid Interface Sci*. 1996;180(1):135-143. doi:https://doi.org/10.1006/jcis.1996.0283
10. Graslund S, Nordlund P, Weigelt J, et al. Protein production and purification. *Nat Methods*. 2008;5(2):135-146. doi:10.1038/nmeth.f.202
11. Paraskevopoulou V, Falcone FH. Polyionic Tags as Enhancers of Protein Solubility in Recombinant Protein Expression. *Microorganisms*. 2018;6(2):47. doi:10.3390/microorganisms6020047
12. Lopez-Laguna H, Unzueta U, Conchillo-Sole O, et al. Assembly of histidine-rich protein materials controlled through divalent cations. *Acta Biomater*. 2019;83:257-264. doi:https://doi.org/10.1016/j.actbio.2018.10.030
13. Jiang N, Li H, Sun H. Recognition of Proteins by Metal Chelation-Based Fluorescent Probes in Cells. *Front Chem*. 2019;7(560). doi:10.3389/fchem.2019.00560
14. Raghunath G, Dyer RB. Kinetics of Histidine-Tagged Protein Association to Nickel-Decorated Liposome Surfaces. *Langmuir*. 2019;35(38):12550-12561. doi:10.1021/acs.langmuir.9b01700
15. Uhlen M, Forsberg G, Moks T, Hartmanis M, Nilsson B. Fusion proteins in biotechnology. *Curr Opin Biotechnol*. 1992;3(4):363-369.

420 doi:https://doi.org/10.1016/0958-1669(92)90164-E
421 16. Ledent P, Duez C, Vanhove M, et al. Unexpected influence of a C-terminal-fused His-
422 tag on the processing of an enzyme and on the kinetic and folding parameters. *Febs*
423 *Lett*. 1997;413(2):194-196. doi:10.1016/s0014-5793(97)00908-3
424 17. Majorek KA, Kuhn ML, Chruszcz M, Anderson WF, Minor W. Double trouble-Buffer
425 selection and His-tag presence may be responsible for nonreproducibility of biomedical
426 experiments. *Protein Sci*. 2014;23(10):1359-1368. doi:10.1002/pro.2520
427 18. Booth WT, Schlachter CR, Pote S, et al. Impact of an N-terminal Polyhistidine Tag on
428 Protein Thermal Stability. *ACS Omega*. 2018;3(1):760-768.
429 doi:10.1021/acsomega.7b01598
430 19. Panek A, Pietrow O, Filipkowski P, Synowiecki J. Effects of the polyhistidine tag on
431 kinetics and other properties of trehalose synthase from Deinococcus geothermalis.
432 *Acta Biochim Pol* . 2013;60(2):163-166.
433 20. Araujo A, Oliva G, Henrique-Silva F, Garratt R, Caceres O, Beltramini L. Influence of
434 the Histidine Tail on the Structure and Activity of Recombinant Chlorocatechol 1,2-
435 Dioxygenase. *Biochem Biophys Res Commun*. 2000;272:480-484.
436 doi:10.1006/bbrc.2000.2802
437 21. Deller MC, Kong L, Rupp B. Protein stability: a crystallographer's perspective. *Acta*
438 *Crystallogr Sect F, Struct Biol Commun*. 2016;72(Pt 2):72-95.
439 doi:10.1107/s2053230x15024619
440 22. Flores SS, Nolan V, Perillo MA, Sanchez JM. Superactive beta-galactosidase inclusion
441 bodies. *Colloids Surfaces B Biointerfaces*. 2019;173:769-775.
442 doi:https://doi.org/10.1016/j.colsurfb.2018.10.049
443 23. Nature. Laemmli buffer Background Purpose of the Laemmli buffer Laemmli Buffer
444 Recipe Preparation Recommended Storage Temperature of Laemmli buffer Laemmli
445 buffer References. *Nature*. Published online 1970.
446 24. Lowry OH, Rosebrough NJ, Farr AL, Randall RJ. Protein measurement with the Folin
447 phenol reagent. *J Biol Chem*. 1951;193(1):265-275.
448 http://www.ncbi.nlm.nih.gov/entrez/query.fcgi?cmd=Retrieve&db=PubMed&dopt=Cit
449 ation&list_uids=14907713
450 25. Selvarajan E, Mohanasrinivasan V. Kinetic studies on exploring lactose hydrolysis
451 potential of beta galactosidase extracted from Lactobacillus plantarum HF571129. *J*
452 *Food Sci Technol*. 2015;52(10):6206-6217. doi:10.1007/s13197-015-1729-z
453 26. Lakowicz JR, Kusba J, Wiczk W, Gryczynski I, Szmacinski H, Johnson ML.

Resolution of the conformational distribution and dynamics of a flexible molecule using frequency-domain fluorometry. *Biophys Chem*. 1991;39(1):79-84. http://www.ncbi.nlm.nih.gov/entrez/query.fcgi?cmd=Retrieve&db=PubMed&dopt=Citation&list_uids=2012836

27. Nolan V, Clop PD, Burgos MI, Perillo MA. Dual substrate/solvent- roles of water and mixed reaction-diffusion control of β-Galactosidase catalyzed reactions in PEG-induced macromolecular crowding conditions. *Biochem Biophys Res Commun*. 2019;515(1):190-195. doi:10.1016/j.bbrc.2019.05.081

28. Schuck P. Size-Distribution Analysis of Macromolecules by Sedimentation Velocity Ultracentrifugation and Lamm Equation Modeling. *Biophys J*. 2000;78(3):1606-1619. doi:https://doi.org/10.1016/S0006-3495(00)76713-0

29. Laue TM, Shah BD, Ridgeway TM, Pelletier SL. Computer-aided interpretation of analytical sedimentation data for proteins. In: S.E. Harding, A.J. Rowe JCH (Eds. ., ed. *Analytical Ultracentrifugation in Biochemistry and Polymer Science*. The Royal Society of Chemistry; 1992:90–125.

30. Jacobson RH, Zhang XJ, DuBose RF, Matthews BW. Three-dimensional structure of beta-galactosidase from E. coli. *Nature*. 1994;369(6483):761-766. doi:10.1038/369761a0

31. Broome AM, Bhavsar N, Ramamurthy G, Newton G, Basilion JP. Expanding the utility of beta-galactosidase complementation: piece by piece. *Mol Pharm*. 2010;7(1):60-74. doi:10.1021/mp900188e

32. Ullmann A. One-step purification of hybrid proteins which have β-galactosidase activity. *Gene*. 1984;29(1-2):27-31. doi:10.1016/0378-1119(84)90162-8

33. Abd Elhameed HAH, Hajdu B, Jancso A, et al. Modulation of the catalytic activity of a metallonuclease by tagging with oligohistidine. *J Inorg Biochem*. 2020;206:111013. doi:https://doi.org/10.1016/j.jinorgbio.2020.111013

34. Esen H, Alpdagtas S, Cakar M, Binay B. Tailoring of recombinant FDH: effect of histidine tag location on solubility and catalytic properties of Chaetomium thermophilum formate dehydrogenase (CtFDH). *Prep Biochem Biotechnol*. Published online 2019. doi:10.1080/10826068.2019.1599394

35. Klose J, Wendt N, Kubald S, et al. Hexa-histidin tag position influences disulfide structure but not binding behavior of in vitro folded N-terminal domain of rat corticotropin-releasing factor receptor type 2a. *Protein Sci*. 2004;13(9):2470-2475. doi:10.1110/ps.04835904

36. Chen Z, Li Y, Yuan Q. Study the effect of His-tag on chondroitinase ABC I based on characterization of enzyme. *Int J Biol Macromol*. 2015;78:96-101. doi:10.1016/j.ijbiomac.2015.03.068
37. Sánchez JM, Nolan V, Perillo MA. β-Galactosidase at the membrane-water interface: A case of an active enzyme with non-native conformation. *Colloids Surfaces B Biointerfaces*. 2013;108. doi:10.1016/j.colsurfb.2013.02.019
38. Nolan V, Sanchez JM, Perillo MA. PEG-induced molecular crowding leads to a relaxed conformation, higher thermal stability and lower catalytic efficiency of Escherichia coli beta-galactosidase. *Colloids Surfaces B Biointerfaces*. 2015;136:1202-1206. doi:https://doi.org/10.1016/j.colsurfb.2015.11.003
39. Juers D, Matthews B, Huber R. LacZ beta-galactosidase: Structure and function of an enzyme of historical and molecular biological importance. *Protein Sci*. 2012;21. doi:10.1002/pro.2165
40. Juers D, Jacobson RH, Wigley D, et al. High resolution refinement of beta-galactosidase in a new crystal form reveals multiple metal-binding sites and provides a structural basis for alpha-complementation. *Protein Sci*. 2000;9:1685-1699.
41. Li X, Jiang Y, Chong S, Walt D. Bottom-up single-molecule strategy for understanding subunit function of tetrameric beta-galactosidase. *Proc Natl Acad Sci*. 2018;115:201805690. doi:10.1073/pnas.1805690115
42. Shoemaker G, Juers D, Coombs J, Matthews B, Craig D. Crystallization of beta-Galactosidase Does Not Reduce the Range of Activity of Individual Molecules â€ . *Biochemistry*. 2003;42:1707-1710. doi:10.1021/bi0204138
43. Wu J FM. Hexahistidine (His6)-tag dependent protein dimerization: a cautionary tale. *Acta Biochim Pol*. 1999;46(3):591-599.
44. Amor-Mahjoub M, Suppini J-P, Gomez-Vrielyunck N, Ladjimi M. The effect of the hexahistidine-tag in the oligomerization of HSC70 constructs. *J Chromatogr B Analyt Technol Biomed Life Sci*. 2007;844:328-334. doi:10.1016/j.jchromb.2006.07.031
45. Kenig M, Peternel Š, Gaberc-Porekar V, Menart V. Influence of the protein oligomericity on final yield after affinity tag removal in purification of recombinant proteins. *J Chromatogr A*. 2006;1101(1-2):293-306. doi:10.1016/j.chroma.2005.09.089

Figures

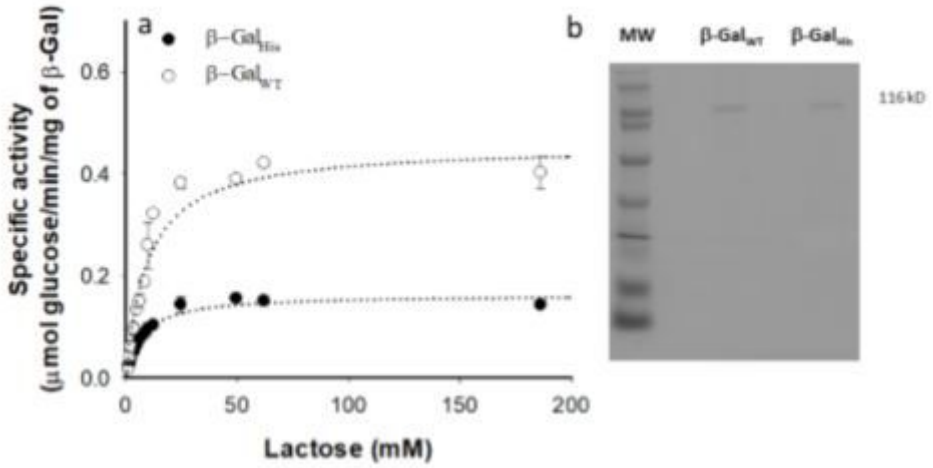

Figure 1

Functional β-Gal properties. a) Specific activity as a function of lactose concentration (β-GalWTwhite symbols, β-GalHis, black symbols). Samples were incubated for 20 min, at 37°C and pH 6.8 and all measurements were carried out in conditions of initial velocity, according to Michaelis-Menten (MM) model. Hyperbolic curves could be adjusted to the experimental points, according to the MM equation. The resulting kinetic parameters are shown in Table 1.b) β-Gals SDS-PAGE.

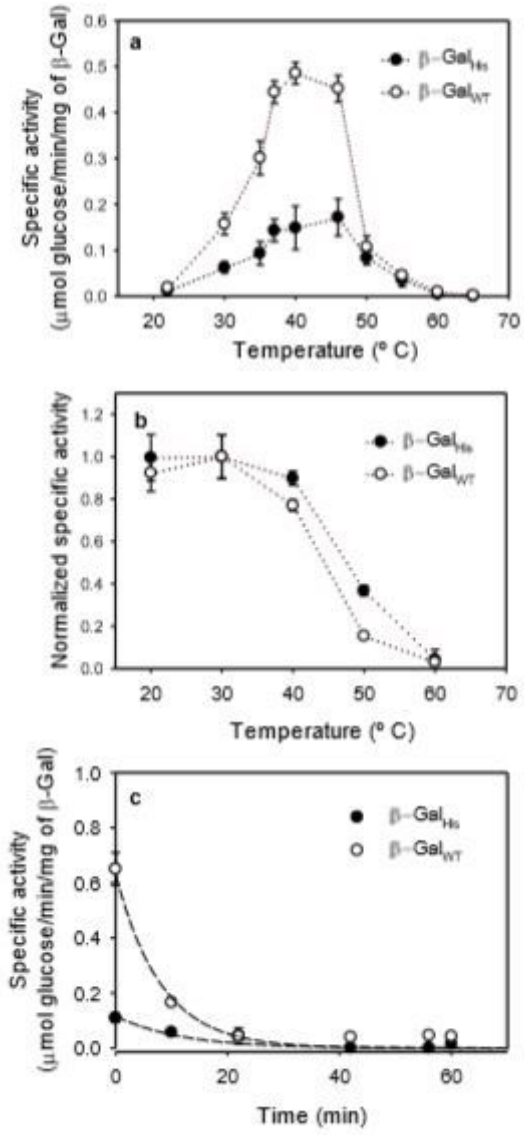

Figure 2

Thermal and temporal inactivation profiles of β-Gals.a) Specific activity measured at the indicated temperature within the range 22ºC - 65ºC. b) β-Gal specific activity measured at 37ºC after preincubation for 20 min. at different temperatures (20-60ºC). In each data set normalization was done with respect to the corresponding specific activity preincubated at 30ºC, which was taken as the unity. c) Catalytic activity was evaluated at 37ºC, pH 6.8 and lactose 200 mM after preheating the proteins (0.01 g/L) at 50ºC during a fix time period (20-60 min). Exponential decay curves (dashed lines) are the fitness to the experimental points (black and white circles) and allowed estimating the half-life times (shown in Table 1).

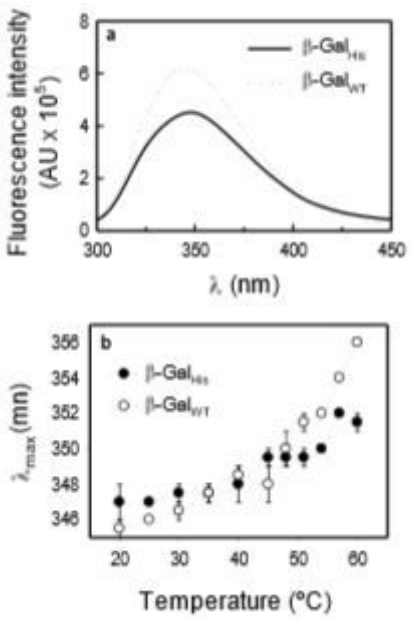

Figure 3

Structural analysis of β-Gals a) Intrinsic fluorescence spectra of of β-GalHis (dotted line) and β-GalWT (full line) proteins at 0.2 g/L at 25°C. b) Effect of temperature on the λmax of β-GalHis (○) and β-GalWT (●).

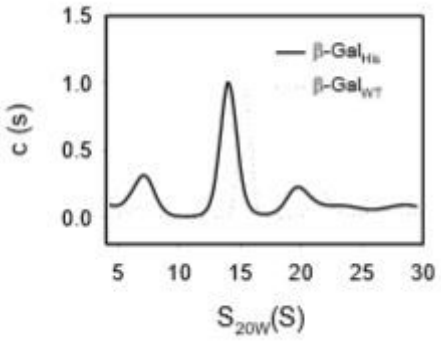

Figure 4

Analytic ultracentrifugation of β-GalHis (full line) and β-GalWT (dotted line)